Analysis of Single and Coupled Rectangular Dielectric Waveguides

ULRICH CROMBACH

Abstract—**Single and coupled rectangular dielectric waveguides are analyzed by means of the mode-matching technique. Dispersion characteristics are given for dominant modes of the inverted stripline and rib waveguides. The propagation constant for E_{11}^{y}-mode of the inverted strip line is found to become less than the lowest limit for guidance above a certain frequency. Influence of frequency and dielectric constant of the rib on the normalized coupling length of two coupled rib waveguides is investigated.**

I. Introduction

A CLASS of waveguides, some of which are shown in Fig. 1, using rectangular dielectric core embedded in one or more layered dielectrics is of increasing interest for millimeter wave or optical integration applications. A number of theoretical studies of their waveguiding properties have been presented in the literature, most of which are based on some effective dielectric constant approximations [1]–[14]. Schlosser *et al.* [15] and Mittra *et al.* [16] were the first to use accurate mode-matching technique for the analysis. Their numerical results agree well with experimental data but their analysis is restricted to the single or coupled image line or to uncoupled rectangular dielectric waveguides, respectively.

In this paper a method used in [17] and [18] for the analysis of microstrip structures by means of mode-matching, is applied to the investigation of single and coupled rectangular dielectric waveguides. The method is applicable to most of the recently proposed dielectric waveguide components such as insulated rectangular image line, inverted stripline or rib waveguide, etc., and allows the investigation of coupling effects between rectangular dielectric waveguides of different cross section. A later publication will show that it is also applicable to the analysis of dielectric ring and disk resonators. The method is exact apart from numerical evaluation where the infinite series have to be approximated. Hence the accuracy of numerical results is limited due to the available storage and computation time.

Since the method is shown in [17], [18] only the main steps of the analysis are described here. Then normalized propagation constant versus normalized free-space wavenumber diagrams are presented for the lowest order modes of inverted strip waveguide, where the dominant mode is either the so called E_{11}^{x}-mode or the E_{11}^{y}-mode. For the latter it is pointed out, that the propagation constant becomes less than the lowest limit for guidance given by theory above a certain value of free-space wavenumber as indicated by [19], [20]. In this case, a closed waveguide model then gives good results for propagation constants of the mode.

Manuscript received November 21, 1980; revised April 1, 1981.

The author is with the Lehrstuhl für Theoretische Elektrotechnik, Technische Hochschule Darmstadt, 61 Darmstadt, Schlossgartenstrasse, 8, West Germany.

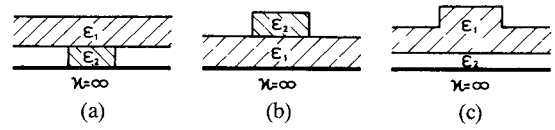

Fig. 1. Cross section of rectangular dielectric waveguides. (a) Inverted stripline. (b) Insulated rectangular image guide. (c) Rib waveguide

Finally dispersion characteristics and normalized coupling length versus normalized free-space wavenumber are presented for the E_{11}^{y}-mode on two coupled rib waveguides backed by a metallic plate, which may be of interest for practical design of integrated waveguide components.

II. Method of Analysis

General geometry of the analyzed structure, which is independent of x_3, is shown in Fig. 2. It is subdivided in partial areas of types I and II which may be considered as parts of parallel-plate lines with layered dielectric homogeneous in x_2-direction. In these areas electromagnetic fields are expanded in infinite series of all eigenmodes of one x_3-dependence. These are derived from two independent types of vector potentials:

$$\vec{A}_m^e = A_{0_m}^e \cdot U_m^e(x_2) \cdot \Phi_m^e(x_1) \cdot f^e(x_3)\vec{e}_1$$
$$\vec{A}_n^h = A_{0_n}^h \cdot I_n^h(x_2) \cdot \Phi_n^h(x_1) \cdot f^h(x_3)\vec{e}_1. \quad (1)$$

The $\Phi_t^{e,h}$ are the eigenfunctions of TM- and TE- modes of the parallel-plate line with layered dielectric [17]. U, I, and f are the related solutions of the separated scalar-wave equation. Using Maxwell's equations, the field components tangential to the area of transitions I–II are then given by

$$\vec{E}_t = -\frac{1}{j\omega\epsilon(x_1)} \sum_{m=1}^{\infty} U_m^e \left[\Phi_m^e f^e \vec{e}_1 + \frac{1}{h_3 K_m^{e2}} \frac{d\Phi_n^e}{dx_1} \frac{df^e}{dx_3} \vec{e}_3 \right] - \frac{1}{h_2} \sum_{n=1}^{\infty} U_n^h \Phi_n^h f^h \vec{e}_3$$

$$\vec{H}_t = \frac{1}{j\omega\mu(x_1)} \sum_{n=1}^{\infty} I_n^h \left[\Phi_n^h f^h \vec{e}_1 + \frac{1}{h_3 K_n^{h2}} \frac{d\Phi_n^h}{dx_1} \frac{df^h}{dx_3} \vec{e}_3 \right] + \frac{1}{h_2} \sum_{m=1}^{\infty} I_m^e \Phi_m^e f^e \vec{e}_3 \quad (2)$$

0018-9480/81/0900-0870$00.75 ©1981 IEEE

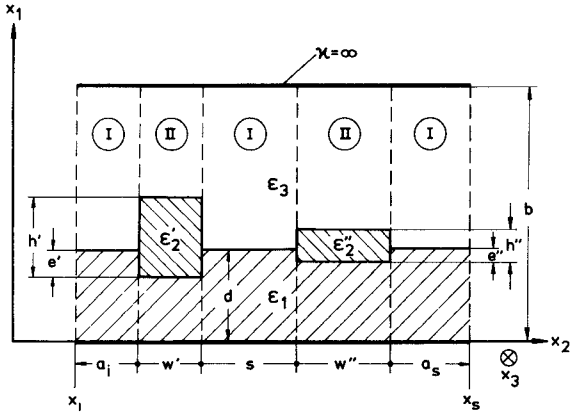

Fig. 2. General geometry of the analyzed structure.

where

$$I_m^e = -A_{0_m}^e \frac{dU_m^e}{dx_2}$$

$$U_n^h = -A_{0_n}^h \frac{dI_n^h}{dx_2}$$

$$K^2 = k^2 - k_{x_1}^2 = \omega^2 \mu(x_1)\epsilon(x_1) - k_{x_1}^2 \qquad (3)$$

(k_{x_1} is transversal wavenumber in one layer of parallel-plate line, h_2, h_3 are metric coefficients of coordinates x_2, x_3).

Now the continuity conditions at the area transitions are satisfied by means of a contradirectional orthogonal expansion [22]. This leads to a coupling matrix V for the amplitudes $U_{m,n}^{e,h}$ and $I_{m,n}^{e,h}$ left and right of the area transitions, summarized to vectors $\vec{U}$ and $\vec{I}$ in areas I and II, as follows:

$$\vec{U}^{\mathrm{I}} = \begin{bmatrix} \vec{U}^e \\ \vec{U}^h \end{bmatrix}^{\mathrm{I}} = V \begin{bmatrix} \vec{U}^e \\ \vec{U}^h \end{bmatrix}^{\mathrm{II}} = V\vec{U}^{\mathrm{II}}$$

$$\vec{I}^{\mathrm{II}} = \begin{bmatrix} \vec{I}^e \\ \vec{I}^h \end{bmatrix}^{\mathrm{II}} = V^T \begin{bmatrix} \vec{I}^e \\ \vec{I}^h \end{bmatrix}^{\mathrm{I}} = V^T\vec{I}^{\mathrm{I}}. \qquad (4)$$

The upper "T" indicates the transposed matrix. In addition transfer diagonal matrices $\boldsymbol{C}$, $\boldsymbol{S}$, $\boldsymbol{R}$, and $\boldsymbol{D}$, which describe the relation between $\vec{U}$ and $\vec{I}$ at two coordinates $x_2 = x_a$ and $x_2 = x_b$ within one area, are defined by

$$\begin{bmatrix} \vec{U} \\ \vec{I} \end{bmatrix}_{x_2 = x_a} = \begin{bmatrix} \boldsymbol{C} & \boldsymbol{S} \\ \boldsymbol{R} & \boldsymbol{D} \end{bmatrix} \begin{bmatrix} \vec{U} \\ \vec{I} \end{bmatrix}_{x_2 = x_b}. \qquad (5)$$

Let a given waveguide structure consist of N_A areas alternate of types I and II and numbered from 1 to N_A. Then by means of the coupling and transfer matrices the continuity conditions are described by a homogeneous linear system of equations for $\vec{U}_p$ and $\vec{I}_p$ ($p = 1 \cdots N_A$) in the middle of the inner areas ($p \neq 1, N_A$) and at the interfaces $x_2 = x_i$ ($p = 1$) and $x_2 = x_s$ ($p = N_A$) in the following manner:

$$\begin{bmatrix} \boldsymbol{C}_1 & \boldsymbol{S}_1 & -\boldsymbol{V}\boldsymbol{C}_2 & -\boldsymbol{V}\boldsymbol{S}_2 & & \boldsymbol{0} & & \boldsymbol{0} \\ \boldsymbol{V}^T\boldsymbol{R}_1 & \boldsymbol{V}^T\boldsymbol{D}_1 & -\boldsymbol{R}_2 & -\boldsymbol{D}_2 & & & & \\ & & \boldsymbol{V}\boldsymbol{C}_2 & \boldsymbol{V}\boldsymbol{S}_2 & -\boldsymbol{C}_3 & \boldsymbol{S}_3 & & \\ \boldsymbol{0} & & \boldsymbol{R}_2 & \boldsymbol{D}_2 & -\boldsymbol{V}^T\boldsymbol{R}_3 & -\boldsymbol{V}^T\boldsymbol{D}_3 & & \boldsymbol{0} \\ & & & & \ddots & & & \\ & & & & \boldsymbol{V}\boldsymbol{C}_{N_A-1} & \boldsymbol{V}\boldsymbol{S}_{N_A-1} & -\boldsymbol{C}_{N_A} & -\boldsymbol{S}_{N_A} \\ & & & & \boldsymbol{R}_{N_A-1} & \boldsymbol{D}_{N_A-1} & -\boldsymbol{V}^T\boldsymbol{R}_{N_A} & -\boldsymbol{V}^T\boldsymbol{D}_{N_A} \end{bmatrix} \begin{bmatrix} \vec{U}_1 \\ \vec{I}_1 \\ \vdots \\ \vec{U}_p \\ \vec{I}_p \\ \vdots \\ \vec{U}_{N_A} \\ \vec{I}_{N_A} \end{bmatrix} = \vec{\boldsymbol{0}}. \qquad (6)$$

Boundary conditions at the margins $x_2 = x_i$ and $x_2 = x_s$ $-\vec{E}_t = \vec{0}$, $\vec{H}_t = \vec{0}$ or "open"—are introduced by striking out ($\vec{U} = \vec{0}$, $\vec{I} = \vec{0}$) or summarizing ($\vec{U} = Z\vec{I}$) the columns related to $\vec{U}_1, \vec{I}_1$ or $\vec{U}_{N_A}, \vec{I}_{N_A}$. In the "open" case the screen at $x_1 = 0, b$ and the dielectric substrate are supposed to extend to infinity in x_2 direction and exponential field decay is assumed in the outer areas. If M^{I} TM- and N^{I} TE-modes are considered in area I and M^{II} and N^{II} in II a quadratic system with $(M^{\mathrm{I}} + N^{\mathrm{I}} + M^{\mathrm{II}} + N^{\mathrm{II}}) \cdot (N_A - 1)$ equations results, of which the zeros of the determinant lead to the unknown propagation constants and field amplitudes for the different waveguide modes. By use of symmetry in x_2-direction the number of equations can be reduced by inserting perfect magnetic or perfect electric conducting walls into the symmetry plane.

III. Numerical Results

Consider a homogeneous waveguide in coordinates $x_1 = y, x_2 = x, x_3 = z$. The height b of the upper screen was chosen to be three times the waveguide height $d+h$ to minimize its influence on the waveguiding properties. The

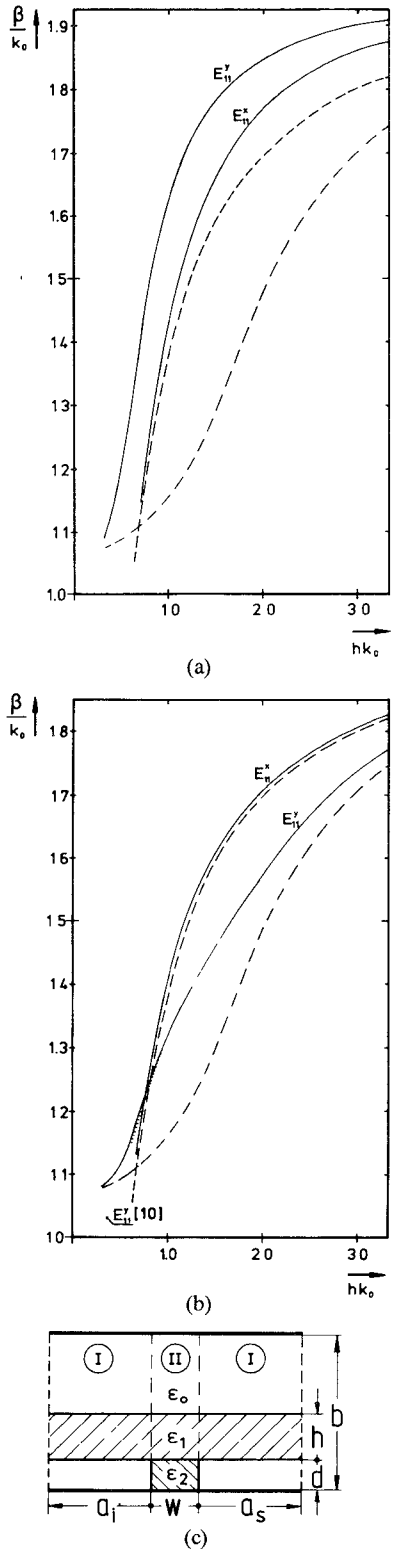

Fig. 3. Normalized propagation constant β/k_0 (solid lines) of E_{11}^y- and E_{11}^x-modes of inverted stripline and normalized separation parameter K/k_0 (3) of dominant TE-eigenmode (dashed) and TM-eigenmode (dash–dotted) in the outer subarea I. $d=h=0.167\ b$, $w=0.42\ b$, $a_l=a_s=\infty$. Number of eigenmodes: 12 TM, 11 TE in I and II. (a) $\epsilon_1=\epsilon_2=3.8\ \epsilon_0$. (b) $\epsilon_1=3.8\ \epsilon_0$, $\epsilon_2=2.1\ \epsilon_0$. ($a_l=a_s=5.0$ W for β/k_0 below the dashed line, the lateral margin of the waveguide is then a perfect electric conductor.)

number of TE- and TM-eigenmodes necessary for satisfying the continuity conditions at the area of transitions and, therefore, the computation time increases with increasing

TABLE I
NORMALIZED PROPAGATION CONSTANT β/k_0 ($k_0=2\pi/\lambda_0$, FREE-SPACE WAVENUMBER) OF E_{11}^y-MODE AND COMPUTATION TIME t FOR CALCULATION OF THE DETERMINANT (6); $d=h=0.167$ b; $w=0.42$ b; $a_l=a_s=\infty$; $hk_0=1.0$; $\epsilon_1=\epsilon_2=3.8\ \epsilon_0$.

	Number of TM/TE-eigenmodes in area I and II					
	1/0	2/1	4/3	6/5	10/9	22/21
β/k_0	1.6560	1.6350	1.6286	1.6318	1.6320	1.6326
t [ms]	6	11	23	37	66	215

ratio $b/(h+d)$. The preceding consideration seemed to be a good compromise in the investigated frequency range. For propagation constants near cutoff, it is not sufficient. Computation time for evaluating the determinant (6) and normalized propagation constant β/k_0 of E_{11}^y-mode on inverted strip guide for various numbers of eigenmodes are given in Table I. Fig. 3(a) and (b) show the normalized propagation constant β/k_0 versus the normalized free-space wavenumber hk_0 for the dominant E_{11}^y- and E_{11}^x-modes of two inverted-strip waveguides with different dielectric constant ϵ_2 of the strip. For exponential field decay in x-direction in the outer subarea I the normalized propagation constant must solve the unequality

$$\beta^2/k_0^2 > K_{\max}^2/k_0^2.$$

$K_{\max}$ is the separation parameter of the dominant eigenmode in the outer area (3).

For the waveguide in Fig. 3(a) with $\epsilon_1=\epsilon_2$ the E_{11}^y-mode is dominant in the whole frequency range. The normalized propagation constant for both the E_{11}^y- and E_{11}^x-modes exceeds the normalized separation constant $K^{e,h}/k_0$ of the dominant TE- and TM-eigenmodes in the outer waveguide area I. For $\epsilon_2<\epsilon_1$ (Fig. 3(b)) a crossover occurs for the plots of propagation constants of E_{11}^y- and E_{11}^x-modes. The propagation constant of E_{11}^y-mode becomes less than the separation parameter of dominant TE-eigenmode above $hk_0=0.8$. Thus representation of E_{11}^y-mode in terms of eigenmodes of a parallel-plate line, which is infinite in x-direction, is no longer valid. At least one TE-eigenmode would be included with nonvanishing fields for $x\to\infty$. Propagation constants of the mode in this part of the frequency range have, therefore, been calculated using a closed waveguide model with perfect electric conducting walls at the lateral margins five times the strip width away from strip center. Field investigations showed that this should be a valid approximation for the open waveguide because field strength at the lateral screen is negligibly small.

In addition the influence of TE-eigenmodes on the propagation constants of E_{11}^y-mode is shown in Table II. The table gives various values if only TM-eigenmodes are considered in field representation against the values calculated with the complete set of eigenmodes. As to be seen from the table the deviation is small and vanishes with increasing frequency. This may explain why excellent agreement within the accuracy of drawing has been found for $hk_0>0.9$

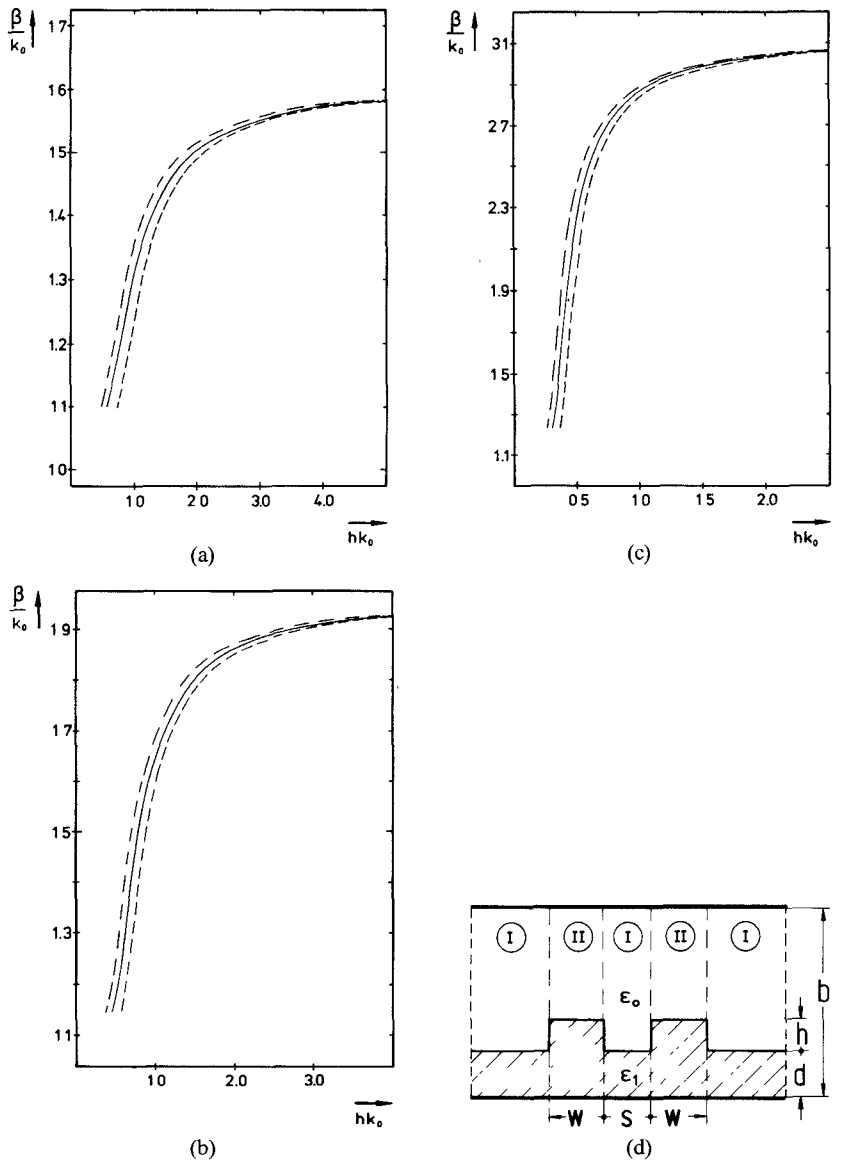

Fig. 4. Normalized propagation constant β/k_0 of $E^y_{11_{even}}$-mode (dash–dotted line) and $E^y_{11_{odd}}$-mode (dashed) of two coupled rib waveguides and normalized propagation constant of E^y_{11}-mode (solid) of single rib waveguide ($s\rightarrow\infty$). $d=h=0.167\ b$, $w=0.333\ b$, $s=0.167\ b$. Number of modes: 12 TM, 11 TE in I and II. (a) $\epsilon_1=2.56\ \epsilon_0$. (b) $\epsilon_1=3.8\ \epsilon_0$. (c) $\epsilon_1=9.6\ \epsilon_0$.

for the waveguide in Fig. 3(b) between the results of this theory and the effective dielectric constant approach [10] (various values given in Table II). The latter ignores the presence of higher order TM- and of TE-eigenmodes.

Figs. 4(a)–(c) present the dispersion characteristics for E^y_{11}-mode on single and coupled rib waveguide backed by a metallic plate versus the normalized free-space wavenumber hk_0 for three values of dielectric constant ϵ_1 of the rib. The propagation constants of both the $E^y_{11_{even}}$- and $E^y_{11_{odd}}$-mode of the coupled waveguide increase quickly near cutoff and approach the propagation constant of uncoupled E^y_{11}-mode. A comparison between the Figs. 4(a)–(c) shows that the deviation is smaller for higher ϵ_1. With increasing frequency or dielectric constant ϵ_1 the coupling between the two waveguides decreases as to be seen from Fig. 5. It shows the dependence on normalized free-space wavenumber hk_0 of normalized coupling length $L/h=\pi/(h(\beta_{even}-\beta_{odd}))$ needed for total power exchange between the two waveguides. The higher the normalized wavenumber or the dielectric constant of the waveguide the higher is the coupling length.

TABLE II
NORMALIZED PROPAGATION CONSTANT β/k_0 OF E^y_{11} = MODE OF INVERTED STRIPLINE IN FIG. 3.

		hk_0 0.833	1.667	2.50	3.333
TM/TE-modes in I and II	12/11	1.2442	1.4959	1.6687	1.7725
	12/0	1.2474	1.4974	1.6686	1.7722
Eff. ε Method		1.2499	1.4987	1.6721	1.7729

β/k_0

Numerical calculations have been carried out in Fortran

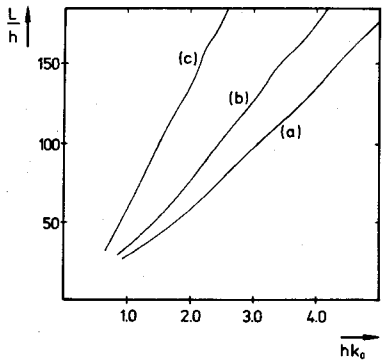

Fig. 5. Normalized coupling length $L/h=\pi/(h(\beta_{even}-\beta_{odd}))$ of the rib waveguides in Fig. 4. (a) $\epsilon_1=2.56\ \epsilon_0$. (b) $\epsilon_1=3.8\ \epsilon_0$. (c) $\epsilon_1=9.6\ \epsilon_0$.

on a IBM 370/168 computer at the "Hochschulrechenzentrum der Technischen Hochschule Darmstadt", Darmstadt, Germany.

IV. Conclusion

A method is described which is applicable to the investigation of the influence of material constants and waveguide dimensions on the propagation constants and fields of waves on most of the commonly used single or coupled rectangular dielectric waveguides.

Numerical data has been presented for rib waveguide and inverted strip waveguide. For the latter special attention has been given to the restriction of guidance for a certain value of dielectric constant.

Acknowledgment

The author wishes to thank Prof. Dr. -Ing. G. Piefke and the members of his staff for helpful discussions and reading the manuscript, and Dr. Ing. H. Brandis for the introduction to some useful Fortran subroutines.

References

[1] W. Schlosser and H. G. Unger, "Partially filled waveguides and surface waveguides of rectangular cross section," in *Advances of Microwaves*, vol. 1. New York: Academic Press, 1966, pp. 319–387

[2] J. E. Goell, "A circular-harmonic computer analysis of rectangular dielectric waveguides," *Bell Syst. Tech. J.*, vol. 48, pp. 2133–2160, Sept. 1969

[3] E. A. J. Marcatili, "Dielectric rectangular waveguide and directional coupler for integrated optics," *Bell Syst. Tech. J.*, vol. 48, pp. 2071–2102, Sept. 1969

[4] R. M. Knox, "Dielectric waveguide integrated circuits—An overview," *IEEE Trans. Microwave Theory Tech.*, vol. MTT-24, pp. 806–814, Nov. 1976

[5] H. Kogelnik, "An introduction to integrated optics," *IEEE Trans. Microwave Theory Tech.*, vol. MTT-23, pp. 2–16, Jan. 1975

[6] S. Bhooshan and R. Mittra, "Multimode waveguide components for millimeter-wave integrated circuits," *Arch. Elektron. Übertragun.*, vol. 34, no. 1, pp. 27–29, Jan. 1980

[7] S. Shindo and T. Itanami, "Low-loss rectangular dielectric image line for millimeter-wave integrated circuits," *IEEE Trans. Microwave Theory Tech.*, vol. MTT-26, pp. 747–751, Oct. 1978

[8] R. Rudokas and T. Itoh, "Passive millimeter wave IC components made of inverted strip dielectric waveguides," *IEEE Trans. Microwave Theory Tech.*, vol. MTT-26, pp. 978–981, Dec. 1976

[9] W. V. McLevige, T. Itoh, and R. Mittra, "New waveguide structures for millimeter-wave and optical integrated circuits," *IEEE Trans. Microwave Theory Tech.*, vol. MTT-23, pp. 788–794, Oct. 1975

[10] T. Itoh, "Inverted strip dielectric waveguide for millimeter-wave integrated circuits," *IEEE Trans. Microwave Theory Tech.*, vol. MTT-24, pp. 821–827, Nov. 1976

[11] R. M. Knox and P. P. Toulios, "Integrated circuits for the millimeter through optical frequency range," presented at Symp. Submillimeter Waves, New York, NY, Mar. 1970

[12] R. Pregla, "A method for the analysis of coupled rectangular dielectric waveguides," *Arch. Elektron. Übertragung.*, vol. 28, no. 9, pp. 349–357, Sept. 1974

[13] K. Ogusu, "Numerical analysis of rectangular dielectric waveguide and its modification," *IEEE Trans. Microwave Theory Tech.*, vol. MTT-25, pp. 874–885, Nov. 1977

[14] P. Gelin, S. Toutain, and J. F. Legier, "New analytical model for rectangular image guide," *Electron. Lett.*, vol. 16, pp. 442–444, May 1980

[15] K. Solbach and I. Wolff, "The electromagnetic fields and the phase constants of dielectric image lines," *IEEE Trans. Microwave Theory Tech.*, vol. MTT-26, pp. 266–274, Apr. 1978

[16] R. Mittra, Y. L. Hou, and V. Jamnejad, "Analysis of open dielectric waveguides using mode-matching technique and variational methods," *IEEE Trans. Microwave Theory Tech.*, vol. MTT 28, pp. 36–43, Jan. 1980

[17] H. Brandis, "Wellen auf einfachen and gekoppelten geschirmten Streifenleitungen als Grundlage zur Analyse von Streifenleitungsübergängen," Dissertation, Technische Hochschule Darmstadt, Germany, D 17, 1978

[18] H. Brandis and U. Crombach, "Resonanzen von Ring- und Scheibenresonatoren in Streifenleitungstechnik," *Frequenz*, vol. 34, pp. 284–287, Oct. 1980

[19] A. A. Oliner, and S. T. Peng, "A new class of leaky modes on dielectric waveguides for millimeter waves," in *Proc. Int. URSI-Symp. Electromagnetic Waves* (Munich, Germany), 1980

[20] ——, "Leakage and resonance effects on strip waveguides for integrated optics," *Trans. IECE Jap.*, vol. E 61, pp. 151–154, Mar. 1978

[21] H. Hönl, A. W. Maue, and K. Westphal, *Theorie der Beugung, Handbuch der Physik*. Berlin, Germany Springer Verlag, 1961

[22] G. Piefke, *Feldtheorie III*. Mannheim, Germany: Bibliographisches Institut, 1977

Ulrich Crombach was born in Fellingshausen, Hessen, West Germany, on June 13, 1954. He received the Dipl. Eng. degree from Technische Hochschule Darmstadt, Darmstadt, West Germany, in 1978.

Since 1978, he has been employed as a Research Assistant in the Department of Communication Engineering, Technische Hochschule Darmstadt, where he is engaged in the theoretical investigation of waveguiding properties of rectangular dielectric waveguides.